

Multi-Feature Extraction with Ensemble Network for Tracing Chronic Retinal Disorders

Muhammad Zubair Khan¹, Yugyung Lee², Arslan Munir³ and Muazzam Ali Khan⁴

Abstract—The retina manifests a vital role in tracing chronic retinal disorders. It is located near the optic nerve that transforms the captured light into neural signals. The most prominent chronic eye diseases exhibit themselves in the retina. The analysis of a retina for detecting disease symptoms is quite challenging. Most of the prior methods developed using shallow and deep learning algorithms primarily emphasized single feature extraction for disease diagnosis. The underlying article has designed an ensemble network for extracting multiple retinal features using a single comprehensive platform. It includes a set of models that reflect feature-based needs to prevent intensity loss, micro-vessels overlap, and data redundancy. The proposed method has experimented with prominent benchmark datasets developed for vessels tree, optic disc/cup, and arteries/veins extraction. It is also compared with other methods and achieved promising results. Our platform is helpful for physicians to trace the variations in the retina of subjects facing chronic retinal disorders.

Index Terms—deep learning, e-health, image analysis, retinal features, semantic segmentation.

I. INTRODUCTION

The advancement of AI algorithms has inspired researchers and scientists to apply these techniques in medical diagnosis, monitoring, and treatment. A diverse range of methods are designed to target a set of medical challenges. The effort is conducted to develop minimalistic solutions with reduced computational complexities in medical image analysis. The core emphasis is to localize the anatomical structures and categorize each pixel in a pre-defined set of classes, a critical step towards the image-guided diagnosis. The publicly available shared pool of resources, including datasets, algorithms, and source code, has motivated and appreciated the deep learning community to contribute in applied optics. It is found that these techniques have provided a solid foundation in tracing chronic ocular disorders such as diabetic retinopathy (DR), hypertensive retinopathy (HR) and glaucoma [1]–[7].

These disorders can affect both central and peripheral vision and are prominent in subjects with diabetes, hypertension, and intraocular pressure. The DR creates a blockage in vessels caused by an increased amount of blood glucose. It prevents the smooth supply of oxygen and essential nutrients from

nourishing the human retina. In HR, chronic hypertension results in arterial and venous occlusion. The extended pressure in arteries and veins ruptures the vessels and causes blood and other fluids to enter the retina. The study conducted in [8] showed that the subjects with retinopathy are potentially at a high risk of vision loss, ischemic stroke, and heart failure.

The intraocular pressure in glaucoma, developed by aqueous humor, results in optic nerve deterioration. It produces blind spots in the visual field and gradually progresses into permanent blindness. Detecting symptoms of these ocular disorders at an early stage through retinal features variation is vital to prevent vision loss. The initial step to analyze the root cause is to precisely segment the retinal features. Common symptoms reflected through retinal features include neovascularization, microaneurysms, arterial and venous occlusion, optic nerve damage, and change in the optic disc (OD) to optic cup (OC) ratio. The underlying article has proposed an ensemble network that can segment multiple features for detecting early symptoms of retinal diseases. The main contribution of this article includes the following:

- 1) A multi-feature extraction algorithm is proposed to trace the symptoms of chronic retinal disorders.
- 2) The region of interest and feature to extract influence the training mode and model selection.
- 3) The method produces a context-aware vessels tree, prevents artery/vein overlapping, and eliminates redundant pixels for effective optic disc/cup extraction.
- 4) The method is evaluated on benchmark datasets publicly available with different focal points and dimensions.

II. RELATED WORK

Deep semantic segmentation has a vital role in medical image analysis. It extracts the regions of interest required for medical diagnosis. A core concept is to effectively label every pixel to its corresponding class and elevate the system precision. Among several architectural solutions proposed by the AI community, the U-Net model [9] is the most prominent technique applied for medical image analysis. It is capable of operating with limited data samples. In [10], a method to analyze non-trivial pathologies with an effective response towards the central vessel reflex phenomenon is highlighted. A deformable U-Net architecture [11] is developed to capture the context knowledge by integrating low and high-end feature maps. The authors of [12] have offered a deeper architectural version to reduce the vanishing gradient problem with adequate feature representations. The method applied the residual and recurrent blocks along with the baseline model proposed

¹Muhammad Zubair Khan, School of Computing and Engineering, University of Missouri-Kansas City, Kansas City, USA (mkzb3@mail.umkc.edu)

²Yugyung Lee, School of Computing and Engineering, University of Missouri-Kansas City, Kansas City, USA (leeyu@umkc.edu)

³Arslan Munir, Department of Computer Science, Kansas State University, Manhattan, USA (amunir@ksu.edu)

⁴Muazzam Ali Khan, Department of Computer Science, Quaid-i-Azam University, Islamabad, Pakistan (muazzam.khattak@qau.edu.pk)

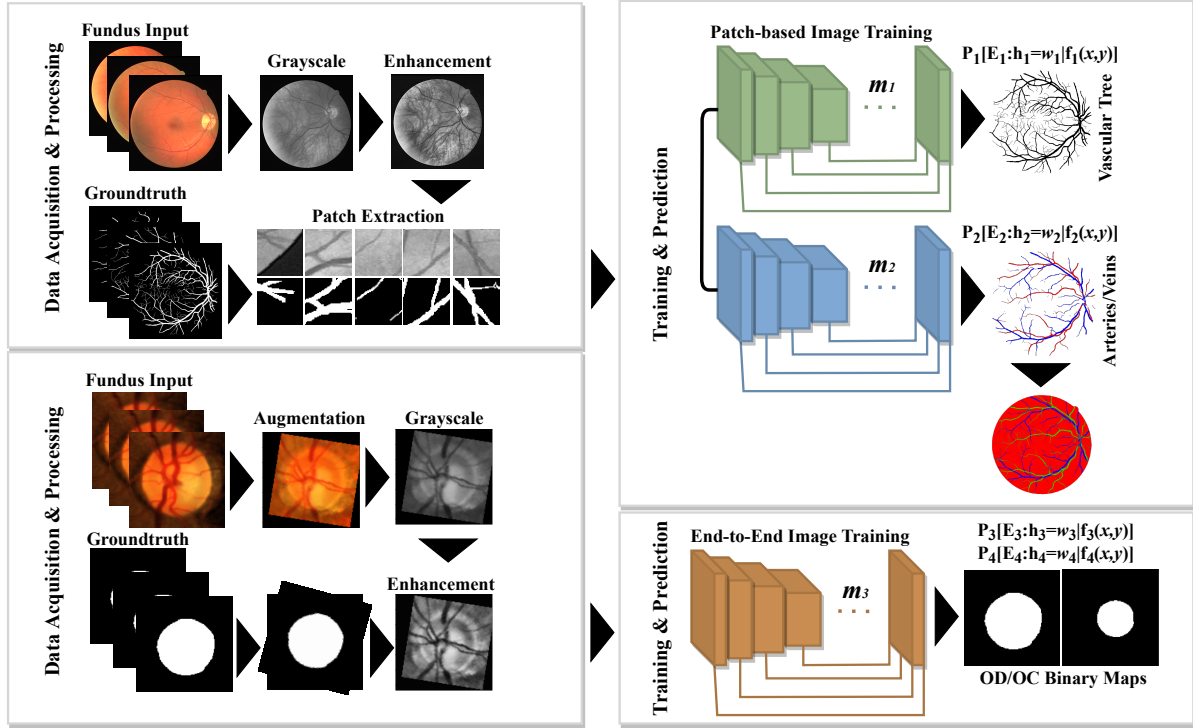


Fig. 1. The context view of the proposed deep ensemble network. The figure depicts the extraction of multiple retinal features.

in [9]. A CU-Net model is designed in [13] to perform medical image segmentation. In [14], a bi-directional attention block adaptively learns the image features by capturing the correlation between pixels.

A cascaded network [15] used both the local and global context for producing feature maps. The LadderNet with adjacent encoder-decoder path pairs is presented in [16]. The authors of [17] have designed an IterNet, a modified U-Net model with an iterative design pattern to semantically segment medical records. In [18], the authors defined a UNet++ model. It is a multi-depth U-Net architecture with a novel pruning method for rapid inferencing. A hard attention network [19] has dynamically distributed the regions to localize the vessels independently using an attention mechanism. The context-encoder network proposed in [20] is an effort to reduce the spatial loss caused by max-pooling and stride operations. It has applied residual multi-kernel pooling and dense atrous convolutions. The residual U-Net was developed to see the impact of skip-connections on deep network architectures. It is an extension to a fully convolutional network with short skip-connections and residual blocks [21]. In [22] the authors applied a multi-scale network with a specialized feature extractor for data-driven DR analysis. The SDL for histogram-based segmentation is used in [23].

In [24], a transfer learning approach for an optic disc/cup segmentation is proposed. The method is operated with the partial weights obtained by training an attention U-Net. These weights are later adjusted with an unseen dataset for retinal disease detection. A learning system for glaucoma detection

is proposed in [25]. Two distinct fuzzy models are defined for optic cup and optic disc localization; the optic disc/cup ratio is also measured to assess the glaucoma stage. [26] defined a self-supervised pre-training technique for reducing data scarcity and provided a multi-modal solution for medical image analysis. In [27], a novel spatial attention module is designed to perform an adaptive feature refinement process. The technique developed in [28] emphasized a graphical structure of vessels to build a strong tie between adjacent pixels. The method transformed the neural graph model into a unified network to exploit both local and global representations to improve segmentation accuracy. The model proposed in [29] has used multi-scale input to achieve multi-sized receptive fields with a U-shaped convolutional network and multi-label function for Optic disc/cup segmentation. A dual-residual stream-based semantic model is developed in [30] for retinopathy diagnosis. It comprises internal and outer residual skip-paths to assure feature re-use and produce direct spatial edge information.

[31] has used image-level annotations to detect lesions for screening diabetic retinopathy. A SeqNet model is developed in [32] for vessels segmentation and classification into arteries and veins. [33] has applied a three-stage model to separate thick vessel from thin vessel. A method proposed in [34] has developed a bi-modular clinical decision system for vessels and optic nerve head analysis. The first module used a support vector machine with RBF kernel for A/V classification and ratio calculation, whereas, the second module performed analysis to detect the symptoms of papilledema. In [35], the

authors designed a method to find the impact of deep learning in predicting hypertension, hyperglycemia, and dyslipidemia. The article [36] analyzed graphs extracted from vascular tree to classify in arteries and veins. The decision is made through graph nodes and graph links. In [37], a pixel classification with inter-subject normalization and intra-image regularization is used for A/V classification. The discriminating properties are captured using first and second-order texture features. The authors in [38] developed the topological graph-theoretic paradigm to distinguish arteries from veins. A multi-layered architecture with a deep residual convolution network is developed to detect the condition of HR patients [39].

III. PROPOSED METHODOLOGY

A. Data Preprocessing

In our experiment, we performed a diverse range of image preprocessing techniques. The images in each dataset are captured using specialized camera sensors with different angles, dimensions, and lighting conditions. The data is standardized for efficient training using series of steps. A green channel is extracted and converted in grayscale to manage the contrast level, equalize the histogram frequency and reduce noise amplification using a contrast-limited adaptive histogram equalization technique. The data is further normalized, and gamma values are corrected with power-law transformation.

B. Network Structure

The ensemble network shown in Fig. 1 contains three distinct models to perform semantic segmentation. Each model is designed to support the system efficacy by responding to an issue a model experiences when dealing with diverse input features without promoting additional computation complexity. The model (m_1) is an encoder-decoder structure with a context restoration unit. It includes bi-directional convolutional LSTM. The unit restores intensity values of degraded input using context information. It enables the model to capture long-range dependencies between pixels and triggers weight sharing for each time-stamp. The model (m_2) contains an attention unit integrated with a U-shaped structure. It produces attention-guided segmentation maps that keep track of micro-vessels. The first part of a network extracts the vessels used by the second part as an input map to emphasize more on the local regions. In model (m_3), a lightweight, minimalistic segmentation model is designed. It has parameters approximately sixteen times less than conventional U-Net architecture. The models essentially involves multiple convolutions and deconvolutions with pooling, batch-normalization, and dropout functions. It is vital to mention that the cost of each model is measured with binary cross-entropy function. The parameters are tuned with adam optimizer by dynamically adjusting the learning rate between 10^{-2} and 10^{-8} . A kernel of size k=3 is used to perform convolutions with the same padding. In up-sampling, we used long skip-connections with identity mappings to create the output as same as the input of the layer and avoid the vanishing gradient problem. The hidden layers are activated with the ReLU function; whereas, a sigmoid

activation function is used in the output layer of each employed model. A leave-one-out and k-fold validation approach is applied for datasets without any visible split. The instruction set for complete training process is provided in Algorithm 1.

Algorithm 1 Multi-Feature Ensemble Network

Notation: color image (\mathbb{I}_{rgb}), channels (α, β, γ), green channel (\mathbb{I}_g), grayscale image (\mathbb{I}_c), enhanced image (\mathbb{I}_e), normalized input (\mathbb{I}_n), sub-sample (\mathbb{I}_s), preprocessed image (\mathbb{I}_p), constant (k), epoch (ε), null (φ), model (m), feature vector (\vec{f}).

```

function Preprocess( $\mathbb{M}$ )
     $\Gamma(\alpha, \beta, \gamma) \leftarrow \text{Split\_Image}(\mathbb{I}_{rgb})$ 
     $\mathbb{I}_g \leftarrow \text{Extract\_Channel}(\Gamma(\alpha, \beta, \gamma))$ 
     $\mathbb{I}_c \leftarrow \text{Convert\_to\_Gray}(\mathbb{I}_g)$ 
     $\mathbb{I}_e \leftarrow \text{Load CLAHE}(\mathbb{I}_c)$ 
     $\mathbb{I}_n \leftarrow \text{Apply Normalization}(\mathbb{I}_e)$ 
for ( $\forall f$  in  $\vec{f}$ ) do
    flag = 1
    if ( $f == \varphi$ ) then
        flag = 0
        break()
    while ( $\mathbb{I}_{rgb} \neq \varphi$ ) do
        if ( $f == (\text{VT} \vee \text{A/V})$ ) then
             $\mathbb{I}_p \leftarrow \text{Preprocess}(\mathbb{I}_{rgb})$ 
            Split  $\mathbb{I}_p$  into  $mxn \mathbb{I}_s$ 
            Retain identical dimension for each  $\mathbb{I}_s$ 
            while ( $(\mathbb{I}_s \neq !1) \wedge (\text{count}(\mathbb{I}_s) \neq !2k)$ ) do
                pop()
            if ( $\mathbb{I}_s$  in VT) then
                 $m_1 \leftarrow \text{Invoke}(m \oplus \text{CRU}) \triangleright (\text{VT extraction})$ 
                for ( $i = 0; i < \varepsilon; i++$ ) do
                     $\hat{m} \leftarrow \text{train}(m_1)$ 
            else if ( $\mathbb{I}_s$  in A/V) then
                 $m_2 \leftarrow \text{Invoke}(m \oplus \text{AU}) \triangleright (\text{A/V extraction})$ 
                for ( $i = 0; i < \varepsilon; i++$ ) do
                     $\hat{m} \leftarrow \text{train}(m_2)$ 
            else
                break()
            else if ( $f == (\text{OC} \vee \text{OD})$ ) then
                Crop  $\mathbb{I}_{rgb}$  around OD
                Perform  $\mathbb{I}_{rgb}$  augmentation
                 $\mathbb{I}_p \leftarrow \text{Preprocess}(\mathbb{I}_{rgb})$ 
                 $m_3 \leftarrow \text{Invoke}(mm) \triangleright (\text{OD/OC extraction})$ 
                for ( $i = 0; i < \varepsilon; i++$ ) do
                     $\hat{m} \leftarrow \text{train}(m_3)$ 
            else
                abort()
     $\vec{f} = \hat{m}.\text{predict}(\mathbf{X}_{test})$ 

```

IV. EXPERIMENTATION

A. System Configuration

The deep architecture with few hidden layers even requires extensive storage and multicore graphical processing units.

TABLE I
FUNDUS IMAGE DATASETS USED IN OUR APPROACH.

Feature	Dataset	Images	Dimension	FOV	Format
Vessels-Tree	DRIVE [40]	40	565×584	45°	TIF
	STARE [41]	20	700×605	35°	PPM
	CHASE-DB1 [42]	28	999×960	30°	JPG
OD/OC	DRISHTI-GS [43]	101	2896×1944	30°	PNG
	RIM-ONE [44]	159	2144×1424	34°	JPG
	DRION-DB [45]	110	600×400	45°	JPG
Artery/Vein	HRF [46]	45	3504×2336	45°	JPG
	LES-AV [47]	22	1620×1444	30°	PNG
	RITE [48]	40	565×584	45°	TIF

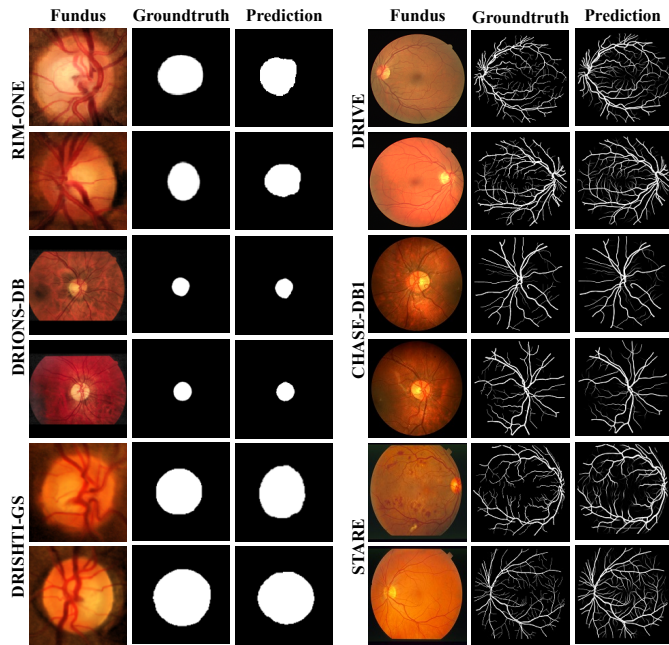


Fig. 2. Extraction of OD/OC and vessels tree with the proposed approach.

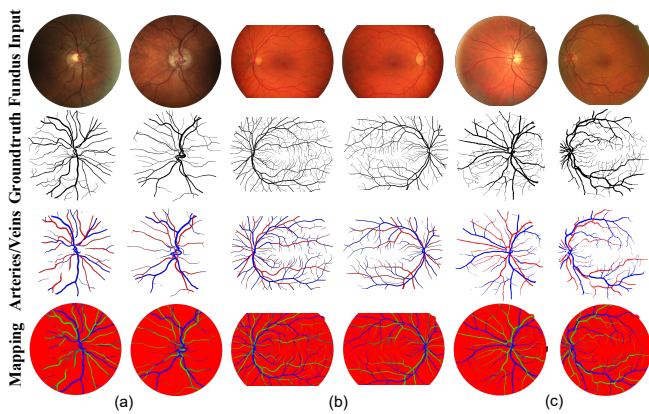


Fig. 3. A/V Extraction, here (a) LES-AV, (b) HRF, (c) RITE

Deploying required resources on-premises makes the training and inference extremely expensive. In this experiment, we have subscribed google colab pro version, a cloud platform designed for AI researchers to make efficient use of high-end resources off-premises for model deployment [49]. Our model is trained with priority-based T4 and P100 GPUs using 25GB RAM. Additional 100GB memory is procured from google cloud storage to meet the secondary memory requirement.

B. Data Collection

The data is acquired from multiple fundus image resources. Each dataset is publicly available for encouraging AI researchers and other scientists to evaluate segmentation techniques designed for glaucoma, diabetic and hypertensive retinopathy detection. In our experiment, we have used three datasets to target each category of a vessel, optic disc/cup, and arteries/veins extraction given in Table I. The data selected is diverse in nature with different dimensions, image quality, focal point, field of view (FOV), format and taken under uneven lighting conditions to mimic the real simulation environment.

TABLE II
EVALUATION OF A PROPOSED METHOD ON BENCHMARK DATASETS.

Feature	Dataset	DICE	IOU	AUC
Vessels-Tree	DRIVE	0.8298	—	0.9887
	STARE	0.8515	—	0.9925
	CHASE-DB1	0.8203	—	0.9890
OD/OC	DRISHTI-GS	0.8940	0.8522	—
	RIM-ONE	0.9567	0.9227	—
	DRION-DB	0.9729	0.9304	—
Artery/Vein	HRF	0.9693	—	0.9780
	LES-AV	0.8258	—	0.9496
	RITE	0.9687	—	0.9868

TABLE III
COMPARISON OF THE PROPOSED METHOD WITH OTHER TECHNIQUES DESIGNED FOR VESSELS TREE EXTRACTION.

Method/Metrics	Dataset		DRIVE		STARE		CHASE-DB1	
	ACC	AUC	ACC	AUC	ACC	AUC	ACC	AUC
Ronneberger [9]	0.9531	0.9755	0.9690	0.9898	0.9578	0.9772		
Yan [50]	0.9542	0.9752	0.9612	0.9901	0.9610	0.9781		
Orlando [51]	—	0.9507	—	—	—	—	0.9524	
Azzopardi [52]	0.9442	0.9614	0.9497	0.9563	0.9387	0.9487		
Zhuo [53]	—	0.9754	—	—	—	—		
Zhuang [16]	0.9561	0.9793	—	—	0.9656	0.9839		
Jin [11]	0.9697	0.9856	0.9729	0.9868	0.9724	0.9863		
Liu [54]	—	0.9798	—	—	—	—		
Liangzhi [17]	0.9573	0.9816	0.9655	0.9851	0.9701	0.9881		
Alom [12]	—	0.9784	—	0.9815	—	—		
Shin [28]	—	0.9801	—	—	—	0.9830		
Alom [12]	0.9556	0.9784	0.9712	0.9914	0.9634	0.9815		
Laibacher [55]	—	0.9714	—	—	—	0.9703		
Mou [56]	—	0.9796	—	—	—	0.9812		
Zhang [57]	0.9476	0.9636	0.9554	0.9748	0.9452	0.9606		
Wang [19]	0.9581	0.9823	0.9673	0.9881	0.9670	0.9871		
Proposed Method	0.9701	0.9887	0.9757	0.9925	0.9738	0.9890		

C. Implementation Results and Comparison

The quantitative analysis of our method is performed using various evaluation metrics, including accuracy, dice-score, an area under the ROC curve (AUC), and intersection over union (IOU). The proposed approach has applied both patch-based and end-to-end image-based training. The precise extraction of features requires adequate preprocessing to fix uneven intensity distribution and noise. The channel with the highest candela/(meter)² value is extracted and transformed into grayscale. The pixel imbalance and noise amplification are reduced by splitting an image into 8×8 tiles and equalizing the histogram to keep intensities uniform across all the bins. The data is normalized for bringing all the intensity values within 0, 1. A lookup chart is created for mapping intensities to their corresponding gamma-corrected values. Our experiment has applied the 80:20 rule on the training data, where 80% of data is kept for training, and 20% is reserved for validation. The number of input samples are different in each dataset highlighted in Table I. Some of the datasets even contain no standard train/test partitioning. The split ratio for unordered data distributions is decided from previous literature.

The choice of training mode and selection of a model depends on the feature to extract. The vascular tree structure and the arteries/veins cover a major portion of an image. The extraction of these features demands a larger area to segment without missing any essential vessel. In optic disc/cup extraction, the ROI is limited to an area around the optic nerve head and the boundary is comparatively well defined; hence, we can easily crop an image to reduce its dimension and restrain our focus to the target region. The proposed method have applied a patch-based approach for vessels and sub-vessels (A/V) extraction. Input samples and groundtruths are divided into 48×48 sub-samples. It has randomly selected 1000 patches from each image with foreground intensities. The network uses these patches to produce segmentation maps equal in dimension to the given input. In optic disc/cup extraction, the area around the optic nerve fiber is cropped for reducing input dimension to boost computational efficiency and used an end-to-end image training approach. The method has applied image augmentation technique before feeding the input to the network with vertical and horizontal flip, rotation at an angle 30°, altering the zoom range by changing coordinate values, and scale shift of 0.1 to the cropped input. After essential preprocessing, the input is provided to the block of training determined by the feature of interest. The evaluation of each extracted feature is given in Table II.

In vessels tree extraction, we can observe that the proposed method for model (m_1) has shown better results than all the related work experimented on DRIVE, STARE, and CHASE-DB1 provided in Table III. The accuracy (ACC) and AUC are used to evaluate and compare our results. It is significant to indicate that using bi-directional convolutional LSTM for intensity restoration helps visualize vessels with enhanced quality and secure context with calculated precision using long-range connections of neighboring pixels. Similarly, model

(m_2) extracts arteries and veins by passing through successive steps of training. The output map of a previous step serves as an input attention map for the next to focus more on local regions and prevent A/V overlapping. Also, it helps in precisely differentiating arteries from veins in a 2D environment. The performance is evaluated with accuracy, AUC, and DICE metrics. Our method has shown a better response on RITE and HRF datasets than recently published work catering to a similar problem, given in Table IV. The extraction of optic disc and cup is performed using DRISHTI-GS, RIM-ONE, and DRION-DB datasets. In Table V, we can see that our method has surpassed by a decent margin to previously conducted work. It has achieved the highest Dice and IOU for the datasets mentioned above. It is important to highlight that model (m_3) has better response for both OD and OC extraction by using least number of parameters (16 times < U-Net architecture). The extraction of multiple features using the proposed ensemble network is depicted in Fig. 2 and Fig. 3. It shows the image, ground truth, and predicted feature map.

TABLE IV
COMPARISON OF THE PROPOSED METHOD WITH OTHER TECHNIQUES FOR ARTERY/VEIN EXTRACTION USING RITE AND HRF DATASETS.

Dataset	RITE			HRF			
	Method/Metrics	ACC	AUC	DICE	ACC	AUC	DICE
Maninis [58]	0.9305	0.9829	—	—	—	—	—
Orlando [51]	0.9508	0.9556	—	0.9464	0.9442	—	—
Yan [59]	0.9582	0.9826	—	0.9449	—	—	—
Galdran [60]	0.9322	0.9847	0.9631	0.9155	0.9424	0.9582	—
Hemelings [61]	0.9479	—	0.9671	0.9681	—	0.9688	—
Proposed Method	0.9617	0.9868	0.9687	0.9698	0.9780	0.9693	—

TABLE V
COMPARISON OF THE PROPOSED METHOD WITH OTHER METHODS DEVELOPED FOR OPTIC DISC/CUP SEGMENTATION.

Dataset	DRISHTI-GS		RIM-ONE		DRION-DB		
	Method/Metrics	DICE	IOU	DICE	IOU	DICE	IOU
Ronneberger [9]	0.8806	0.8487	0.9531	0.8914	0.9688	0.8802	—
Zhou [62]	0.8470	—	0.8530	—	—	—	—
Son [63]	0.8643	0.7748	0.9532	0.9122	0.9685	—	—
Zahoor [64]	—	—	—	—	—	0.8860	—
Fu [65]	0.8618	0.7730	0.9526	0.9114	—	—	—
Wang [66]	0.8580	—	0.8650	—	—	—	—
Gu [20]	0.8818	0.8006	0.9527	0.9115	—	—	—
DRIU [58]	—	—	—	—	0.9725	0.8805	—
Xu [67]	0.8920	0.8230	0.9561	0.9172	—	—	—
Zilly [68]	0.8710	0.8507	0.9413	0.8909	—	—	—
Sevastopolsky [69]	0.8521	0.7515	0.9516	0.8921	0.9426	0.8928	—
Abdullah [70]	—	—	—	—	0.9102	0.8512	—
Al-Bander [71]	0.8282	0.7113	0.9036	0.8289	0.9415	0.8912	—
Shuang [72]	0.8739	0.7808	0.9491	0.9065	—	—	—
Proposed Method	0.8940	0.8522	0.9567	0.9227	0.9729	0.9304	—

V. CONCLUSION AND FUTURE WORKS

In conclusion, we have designed a platform to advance a vision-critical system for tracing chronic eye disorders by extracting retinal features. Each feature is segmented with a specialized semantic network influenced by the region of

interest. The platform used both patch-based and end-to-end image-based training methods applied on benchmark fundus data. The experiment shows that our method has a promising impact in dealing with missing vessels, vessels overlapping, and data redundancy. The concept can be deployed as a unified diagnostic system to early detect the symptoms of glaucoma, diabetic and hypertensive retinopathy. In the future, the proposed platform would be extended for finding the correlation between retinal disorders and systemic diseases like cardiac arrest and alzheimer's disease. Additionally, at an architectural level, we would use the pre-trained models to analyze the platform response for unseen data distributions.

VI. ACKNOWLEDGMENT

The work is funded by the Balaji K. Memorial grant and School of Graduate Studies, UMKC. The responsibility of the research work is on the primary author and does not represent any view from the funding authorities.

REFERENCES

- [1] M. Z. Khan, M. K. Gajendran, Y. Lee, and M. A. Khan, "Deep neural architectures for medical image semantic segmentation: Review," *IEEE Access*, vol. 9, pp. 83 002–83 024, 2021.
- [2] E. Vocaturo and E. Zumpano, "The contribution of ai in the detection of the diabetic retinopathy," in *2020 IEEE International Conference on Bioinformatics and Biomedicine (BIBM)*. IEEE, 2020, pp. 1516–1519.
- [3] M. Z. Khan and Y. Lee, "Screening fundus images to extract multiple ocular features: A unified modeling approach," in *2021 IEEE EMBS International Conference on Biomedical and Health Informatics (BHI)*, 2021, pp. 1–5.
- [4] W. Cao, J. Shan, N. Czarnek, and L. Li, "Microaneurysm detection in fundus images using small image patches and machine learning methods," in *2017 IEEE International Conference on Bioinformatics and Biomedicine (BIBM)*, 2017, pp. 325–331.
- [5] M. Z. Khan and Y. Lee, "Dynamic inductive transfer learning with decision support feedback to optimize retina analysis," in *2021 IEEE 9th International Conference on Healthcare Informatics (ICHI)*, 2021, pp. 93–100.
- [6] A. Singh and W. Kim, "Detection of diabetic blindness with deep-learning," in *2020 IEEE International Conference on Bioinformatics and Biomedicine (BIBM)*, 2020, pp. 2440–2447.
- [7] M. Z. Khan and Y. Lee, "Localization of ocular vessels with context sensitive semantic segmentation," in *2021 IEEE EMBS International Conference on Biomedical and Health Informatics (BHI)*, 2021, pp. 1–5.
- [8] M. F. K. Suri and A. I. Qureshi, "Hypertensive retinopathy and risk of cardiovascular diseases in a national cohort," *Journal of vascular and interventional neurology*, vol. 1, no. 3, p. 75, 2008.
- [9] O. Ronneberger, P. Fischer, and T. Brox, "U-net: Convolutional networks for biomedical image segmentation," in *International Conference on Medical image computing and computer-assisted intervention*. Springer, 2015, pp. 234–241.
- [10] P. Liskowski and K. Krawiec, "Segmenting retinal blood vessels with deep neural networks," *IEEE transactions on medical imaging*, vol. 35, no. 11, pp. 2369–2380, 2016.
- [11] Q. Jin, Z. Meng, T. D. Pham, Q. Chen, L. Wei, and R. Su, "Dunet: A deformable network for retinal vessel segmentation," *Knowledge-Based Systems*, vol. 178, pp. 149–162, 2019.
- [12] M. Z. Alom, C. Yakopcic, M. Hasan, T. M. Taha, and V. K. Asari, "Recurrent residual u-net for medical image segmentation," *Journal of Medical Imaging*, vol. 6, no. 1, p. 014006, 2019.
- [13] A. A. Albishri, S. J. H. Shah, and Y. Lee, "Cu-net: Cascaded u-net model for automated liver and lesion segmentation and summarization," in *2019 IEEE International Conference on Bioinformatics and Biomedicine (BIBM)*, 2019, pp. 1416–1423.
- [14] K. Li, X. Qi, Y. Luo, Z. Yao, X. Zhou, and M. Sun, "Accurate retinal vessel segmentation in color fundus images via fully attention-based networks," *IEEE Journal of Biomedical and Health Informatics*, 2020.
- [15] S. Hussain, S. M. Anwar, and M. Majid, "Brain tumor segmentation using cascaded deep convolutional neural network," in *2017 39th Annual International Conference of the IEEE Engineering in Medicine and Biology Society (EMBC)*. IEEE, 2017, pp. 1998–2001.
- [16] J. Zhuang, "Laddernet: Multi-path networks based on u-net for medical image segmentation," *arXiv preprint arXiv:1810.07810*, 2018.
- [17] L. Li, M. Verma, Y. Nakashima, H. Nagahara, and R. Kawasaki, "Iternet: Retinal image segmentation utilizing structural redundancy in vessel networks," in *The IEEE Winter Conference on Applications of Computer Vision*, 2020, pp. 3656–3665.
- [18] Z. Zhou, M. M. R. Siddiquee, N. Tajbakhsh, and J. Liang, "Unet++: Redesigning skip connections to exploit multiscale features in image segmentation," *IEEE Transactions on Medical Imaging*, vol. 39, no. 6, pp. 1856–1867, 2020.
- [19] D. Wang, A. Haytham, J. Pottenburgh, O. Saeedi, and Y. Tao, "Hard attention net for automatic retinal vessel segmentation," *IEEE Journal of Biomedical and Health Informatics*, vol. 24, no. 12, pp. 3384–3396, 2020.
- [20] Z. Gu, J. Cheng, H. Fu, K. Zhou, H. Hao, Y. Zhao, T. Zhang, S. Gao, and J. Liu, "Ce-net: Context encoder network for 2d medical image segmentation," *IEEE transactions on medical imaging*, vol. 38, no. 10, pp. 2281–2292, 2019.
- [21] D. Li, D. A. Dharmawan, B. P. Ng, and S. Rahardja, "Residual u-net for retinal vessel segmentation," in *2019 IEEE International Conference on Image Processing (ICIP)*. IEEE, 2019, pp. 1425–1429.
- [22] R. Pires, S. Avila, J. Wainer, E. Valle, M. D. Abramoff, and A. Rocha, "A data-driven approach to referable diabetic retinopathy detection," *Artificial intelligence in medicine*, vol. 96, pp. 93–106, 2019.
- [23] K. Shankar, A. R. W. Sait, D. Gupta, S. Lakshmanaprabu, A. Khanna, and H. M. Pandey, "Automated detection and classification of fundus diabetic retinopathy images using synergic deep learning model," *Pattern Recognition Letters*, vol. 133, pp. 210–216, 2020.
- [24] X. Zhao, S. Wang, J. Zhao, H. Wei, M. Xiao, and N. Ta, "Application of an attention u-net incorporating transfer learning for optic disc and cup segmentation," *Signal, Image and Video Processing*, pp. 1–9, 2020.
- [25] R. Ali, B. Sheng, P. Li, Y. Chen, H. Li, P. Yang, Y. Jung, J. Kim, and C. L. P. Chen, "Optic disk and cup segmentation through fuzzy broad learning system for glaucoma screening," *IEEE Transactions on Industrial Informatics*, vol. 17, no. 4, pp. 2476–2487, 2021.
- [26] S. Hervella, L. Ramos, J. Rouco, J. Novo, and M. Ortega, "Multi-modal self-supervised pre-training for joint optic disc and cup segmentation in eye fundus images," in *ICASSP 2020 - 2020 IEEE International Conference on Acoustics, Speech and Signal Processing (ICASSP)*, 2020, pp. 961–965.
- [27] C. Guo, M. Szemenyei, Y. Yi, W. Wang, B. Chen, and C. Fan, "Sa-unet: Spatial attention u-net for retinal vessel segmentation," *arXiv preprint arXiv:2004.03696*, 2020.
- [28] S. Y. Shin, S. Lee, I. D. Yun, and K. M. Lee, "Deep vessel segmentation by learning graphical connectivity," *Medical image analysis*, vol. 58, p. 101556, 2019.
- [29] H. Fu, J. Cheng, Y. Xu, D. W. K. Wong, J. Liu, and X. Cao, "Joint optic disc and cup segmentation based on multi-label deep network and polar transformation," *IEEE Transactions on Medical Imaging*, vol. 37, no. 7, pp. 1597–1605, 2018.
- [30] M. Arsalan, M. Owais, T. Mahmood, S. W. Cho, and K. R. Park, "Aiding the diagnosis of diabetic and hypertensive retinopathy using artificial intelligence-based semantic segmentation," *Journal of clinical medicine*, vol. 8, no. 9, p. 1446, 2019.
- [31] G. Quellec, K. Charrière, Y. Boudi, B. Cochener, and M. Lamard, "Deep image mining for diabetic retinopathy screening," *Medical image analysis*, vol. 39, pp. 178–193, 2017.
- [32] L. Li, M. Verma, Y. Nakashima, R. Kawasaki, and H. Nagahara, "Joint learning of vessel segmentation and artery/vein classification with post-processing," in *Medical Imaging with Deep Learning*. PMLR, 2020, pp. 440–453.
- [33] Z. Yan, X. Yang, and K. T. Cheng, "A three-stage deep learning model for accurate retinal vessel segmentation," *IEEE Journal of Biomedical and Health Informatics*, vol. 23, no. 4, pp. 1427–1436, 2019.
- [34] S. Akbar, M. U. Akram, M. Sharif, A. Tariq, and U. ullah Yasin, "Arteriovenous ratio and papilledema based hybrid decision support system for detection and grading of hypertensive retinopathy," *Computer methods and programs in biomedicine*, vol. 154, pp. 123–141, 2018.
- [35] L. Zhang, M. Yuan, Z. An, X. Zhao, H. Wu, H. Li, Y. Wang, B. Sun, H. Li, S. Ding *et al.*, "Prediction of hypertension, hyperglycemia and

- dyslipidemia from retinal fundus photographs via deep learning: A cross-sectional study of chronic diseases in central china," *Plos one*, vol. 15, no. 5, p. e0233166, 2020.
- [36] B. Dashtbozorg, A. M. Mendonça, and A. Campilho, "An automatic graph-based approach for artery/vein classification in retinal images," *IEEE Transactions on Image Processing*, vol. 23, no. 3, pp. 1073–1083, 2014.
- [37] X. Xu, W. Ding, M. D. Abràmoff, and R. Cao, "An improved arteriovenous classification method for the early diagnostics of various diseases in retinal image," *Computer methods and programs in biomedicine*, vol. 141, pp. 3–9, 2017.
- [38] R. Estrada, M. J. Allingham, P. S. Mettu, S. W. Cousins, C. Tomasi, and S. Farsiu, "Retinal artery-vein classification via topology estimation," *IEEE Transactions on Medical Imaging*, vol. 34, no. 12, pp. 2518–2534, 2015.
- [39] Q. Abbas and M. E. Ibrahim, "Densehyper: an automatic recognition system for detection of hypertensive retinopathy using dense features transform and deep-residual learning," *Multimedia Tools and Applications*, vol. 79, no. 41, pp. 31 595–31 623, 2020.
- [40] J. Staal, M. D. Abràmoff, M. Niemeijer, M. A. Viergever, and B. Van Ginneken, "Ridge-based vessel segmentation in color images of the retina," *IEEE transactions on medical imaging*, vol. 23, no. 4, pp. 501–509, 2004.
- [41] A. Hoover, V. Kouznetsova, and M. Goldbaum, "Locating blood vessels in retinal images by piecewise threshold probing of a matched filter response," *IEEE Transactions on Medical imaging*, vol. 19, no. 3, pp. 203–210, 2000.
- [42] M. M. Fraz, P. Remagnino, A. Hoppe, B. Uyyanonvara, A. R. Rudnicka, C. G. Owen, and S. A. Barman, "An ensemble classification-based approach applied to retinal blood vessel segmentation," *IEEE Transactions on Biomedical Engineering*, vol. 59, no. 9, pp. 2538–2548, 2012.
- [43] J. Sivaswamy, S. Krishnadas, G. D. Joshi, M. Jain, and A. U. S. Tabish, "Drishti-gs: Retinal image dataset for optic nerve head (ohn) segmentation," in *2014 IEEE 11th international symposium on biomedical imaging (ISBI)*. IEEE, 2014, pp. 53–56.
- [44] F. Fumero, S. Alayón, J. L. Sanchez, J. Sigut, and M. Gonzalez-Hernandez, "Rim-one: An open retinal image database for optic nerve evaluation," in *2011 24th international symposium on computer-based medical systems (CBMS)*. IEEE, 2011, pp. 1–6.
- [45] E. J. Carmona, M. Rincón, J. García-Feijoó, and J. M. Martínez-de-la Casa, "Identification of the optic nerve head with genetic algorithms," *Artificial Intelligence in Medicine*, vol. 43, no. 3, pp. 243–259, 2008.
- [46] A. Budai, R. Bock, A. Maier, J. Hornegger, and G. Michelson, "Robust vessel segmentation in fundus images," *International journal of biomedical imaging*, vol. 2013, 2013.
- [47] J. I. Orlando, J. B. Breda, K. Van Keer, M. B. Blaschko, P. J. Blanco, and C. A. Bulant, "Towards a glaucoma risk index based on simulated hemodynamics from fundus images," in *International Conference on Medical Image Computing and Computer-Assisted Intervention*. Springer, 2018, pp. 65–73.
- [48] Q. Hu, M. D. Abràmoff, and M. K. Garvin, "Automated separation of binary overlapping trees in low-contrast color retinal images," in *International conference on medical image computing and computer-assisted intervention*. Springer, 2013, pp. 436–443.
- [49] M. Z. Khan and U. Qamar, "Towards service evaluation and ranking model for cloud infrastructure selection," in *2015 IEEE 12th Intl Conf on Ubiquitous Intelligence and Computing and 2015 IEEE 12th Intl Conf on Autonomic and Trusted Computing and 2015 IEEE 15th Intl Conf on Scalable Computing and Communications and Its Associated Workshops (UIC-ATC-ScalCom)*, 2015, pp. 1282–1287.
- [50] Z. Yan, X. Yang, and K.-T. Cheng, "A three-stage deep learning model for accurate retinal vessel segmentation," *IEEE journal of biomedical and health informatics*, vol. 23, no. 4, pp. 1427–1436, 2018.
- [51] J. I. Orlando, E. Prokofyeva, and M. B. Blaschko, "A discriminatively trained fully connected conditional random field model for blood vessel segmentation in fundus images," *IEEE transactions on Biomedical Engineering*, vol. 64, no. 1, pp. 16–27, 2016.
- [52] G. Azzopardi, N. Strisciuglio, M. Vento, and N. Petkov, "Trainable cosfire filters for vessel delineation with application to retinal images," *Medical image analysis*, vol. 19, no. 1, pp. 46–57, 2015.
- [53] Z. Zhuo, J. Huang, K. Lu, D. Pan, and S. Feng, "A size-invariant convolutional network with dense connectivity applied to retinal vessel segmentation measured by a unique index," *Computer methods and programs in biomedicine*, vol. 196, p. 105508, 2020.
- [54] N. Liu, L. Liu, and J. Wang, "Local adaptive u-net for medical image segmentation," in *2020 IEEE International Conference on Bioinformatics and Biomedicine (BIBM)*. IEEE, 2020, pp. 670–674.
- [55] T. Laibacher, T. Weyde, and S. Jalali, "M2u-net: Effective and efficient retinal vessel segmentation for real-world applications," in *Proceedings of the IEEE/CVF Conference on Computer Vision and Pattern Recognition Workshops*, 2019, pp. 0–0.
- [56] L. Mou, L. Chen, J. Cheng, Z. Gu, Y. Zhao, and J. Liu, "Dense dilated network with probability regularized walk for vessel detection," *IEEE transactions on medical imaging*, vol. 39, no. 5, pp. 1392–1403, 2019.
- [57] J. Zhang, B. Dashtbozorg, E. Bekkers, J. P. Pluim, R. Duits, and B. M. ter Haar Romeny, "Robust retinal vessel segmentation via locally adaptive derivative frames in orientation scores," *IEEE transactions on medical imaging*, vol. 35, no. 12, pp. 2631–2644, 2016.
- [58] K.-K. Maninis, J. Pont-Tuset, P. Arbeláez, and L. Van Gool, "Deep retinal image understanding," in *International conference on medical image computing and computer-assisted intervention*. Springer, 2016, pp. 140–148.
- [59] Z. Yan, X. Yang, and K.-T. Cheng, "Joint segment-level and pixel-wise losses for deep learning based retinal vessel segmentation," *IEEE Transactions on Biomedical Engineering*, vol. 65, no. 9, pp. 1912–1923, 2018.
- [60] A. Galdran, M. Meyer, P. Costa, A. Campilho *et al.*, "Uncertainty-aware artery/vein classification on retinal images," in *2019 IEEE 16th International Symposium on Biomedical Imaging (ISBI 2019)*. IEEE, 2019, pp. 556–560.
- [61] R. Hemelings, B. Elen, I. Stalmans, K. Van Keer, P. De Boever, and M. B. Blaschko, "Artery-vein segmentation in fundus images using a fully convolutional network," *Computerized Medical Imaging and Graphics*, vol. 76, p. 101636, 2019.
- [62] W. Zhou, Y. Yi, Y. Gao, and J. Dai, "Optic disc and cup segmentation in retinal images for glaucoma diagnosis by locally statistical active contour model with structure prior," *Computational and mathematical methods in medicine*, vol. 2019, 2019.
- [63] J. Son, S. J. Park, and K.-H. Jung, "Towards accurate segmentation of retinal vessels and the optic disc in fundoscopic images with generative adversarial networks," *Journal of digital imaging*, vol. 32, no. 3, pp. 499–512, 2019.
- [64] M. N. Zahoor and M. M. Fraz, "Fast optic disc segmentation in retina using polar transform," *IEEE Access*, vol. 5, pp. 12 293–12 300, 2017.
- [65] H. Fu, J. Cheng, Y. Xu, D. W. K. Wong, J. Liu, and X. Cao, "Joint optic disc and cup segmentation based on multi-label deep network and polar transformation," *IEEE transactions on medical imaging*, vol. 37, no. 7, pp. 1597–1605, 2018.
- [66] S. Wang, L. Yu, X. Yang, C.-W. Fu, and P.-A. Heng, "Patch-based output space adversarial learning for joint optic disc and cup segmentation," *IEEE transactions on medical imaging*, vol. 38, no. 11, pp. 2485–2495, 2019.
- [67] Y.-l. Xu, S. Lu, H.-x. Li, and R.-r. Li, "Mixed maximum loss design for optic disc and optic cup segmentation with deep learning from imbalanced samples," *Sensors*, vol. 19, no. 20, p. 4401, 2019.
- [68] J. Zilly, J. M. Buhmann, and D. Mahapatra, "Glaucoma detection using entropy sampling and ensemble learning for automatic optic cup and disc segmentation," *Computerized Medical Imaging and Graphics*, vol. 55, pp. 28–41, 2017.
- [69] A. Sevastopolsky, "Optic disc and cup segmentation methods for glaucoma detection with modification of u-net convolutional neural network," *Pattern Recognition and Image Analysis*, vol. 27, no. 3, pp. 618–624, 2017.
- [70] M. Abdullah, M. M. Fraz, and S. A. Barman, "Localization and segmentation of optic disc in retinal images using circular hough transform and grow-cut algorithm," *PeerJ*, vol. 4, p. e2003, 2016.
- [71] B. Al-Bander, B. M. Williams, W. Al-Nuaimy, M. A. Al-Taee, H. Pratt, and Y. Zheng, "Dense fully convolutional segmentation of the optic disc and cup in colour fundus for glaucoma diagnosis," *Symmetry*, vol. 10, no. 4, p. 87, 2018.
- [72] S. Yu, D. Xiao, S. Frost, and Y. Kanagasingam, "Robust optic disc and cup segmentation with deep learning for glaucoma detection," *Computerized Medical Imaging and Graphics*, vol. 74, pp. 61–71, 2019.